

doi:10.15199/48.2017.02.46

## Temperature distribution on a quad-core microprocessor and quad-core microprocessor / heat sink structure

**Abstract.** In this paper temperature distribution in a heat-sink was analyzed. Laboratory models of quad-core microprocessors (source of heat) were designed and fabricated. They were realized as four properly connected and supplied thick-film resistors, screen-printed on alumina substrate. Temperature distribution was monitored using thermovision camera.

**Streszczenie.** W niniejszym opracowaniu przeprowadzono analizę rozptyłu ciepła na radiatorze. Zaprojektowano i wykonano w tym celu laboratoryjny model procesora czterordzeniowego (źródło ciepła). Został on zrealizowany w postaci czterech odpowiednio połączonych rezystorów grubowarstwowych naniesionych techniką sitodruku na podłoża alundowe. Rozkład temperatury był monitorowany za pomocą kamery termowizyjnej. (Rozpływ ciepła na czterordzeniowym mikroprocesorze oraz na granicy mikroprocesora i radiatora).

**Keywords:** heat sink, heater, resistor, microprocessor.

**Słowa kluczowe:** radiator, grzejnik, mikroprocesor.

### Introduction

Measurements of temperature distribution on the processor/heat-sink interface as well as on the heat-sink area are presented in this paper. The following article is also introduction to research of processing power optimization of fast processors with information about thermal open system consisting of a the integrated circuit and the environment. The structures with four properly connected and supplied thick-film resistors, intended to simulate quad-processor (the use of such a structure makes it possible to simulate the heat that is transferred to the heat sink of computer [1]), were made. ESL-2611-SP (10  $\Omega/\square$  sheet resistance) and DuPont 2021 (100  $\Omega/\square$  sheet resistance) thick-film resistive inks were used. Four 14.00×11.87 mm<sup>2</sup> resistors were screen-printed and fired according to ink manufacturer data sheet [2] on 37.5×32×0.26 mm<sup>3</sup> alumina substrate. Mask pattern is presented in Fig. 1. The values of heaters' resistances are shown in Table 1, whereas the thermal model of quad-core microprocessor is given in Fig. 2.

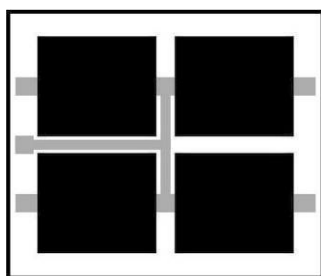


Fig. 1. Mask pattern of heaters

Table 1. Fabricated structures - terminology and used paste

Structure names	1.ESL 2611-SP	2.DuPont 2021
Paths/Pads	DuPont 6146 (Pd-Ag)	
Resistance of heaters [ $\Omega$ ]	1. 45.44	1. 85.90
	2. 44.03	2. 87.96
	3. 45.69	3. 87.54
	4. 43.61	4. 85.63

### Controller

The structure and planar dimensions of four resistors were designed to simulate the thermal model of quad-core microprocessor. In order to measure the effect of heating of selected resistors (processor cores) on the heat-sink the appropriate driver was designed and fabricated [3]. This

controller allows selective heating of particular resistors - this means that it is possible to heat one, two, three or four resistors at the same time. The numbering of heated elements is consistent with Fig. 3.

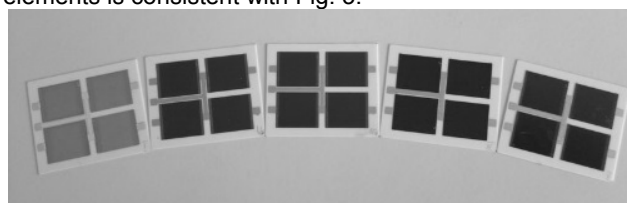


Fig. 2. Fabricated resistors (heaters) on alumina substrates

The controller permits to control the heating (supplying) time of heaters. The trial version of the driver software allows setting the heating time in the range between 10 and 2500 seconds in increments of 10 seconds.

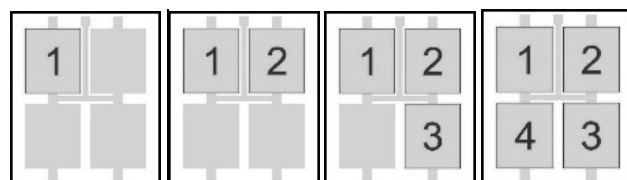


Fig. 3. Numbering of heated elements used during measurement (four possible configurations - from left to right "K1", "K2," "K3" and "K4")

### Thermovision measurements

The infrared ThermoVision A40M FLIR Systems was used for measurement of temperature distribution on the surface of thermal model of quad-core microprocessor as well as on a heat-sink. Temperature was measured onto substrate side opposite to the heaters (resistors). Tested structures were placed into black-painted box with volume of about 0.5 m<sup>3</sup>, in order to prevent from entering visible light and infrared radiation from the outside. The measuring place enabled also avoid impact of the air blast on the measurement results. Therefore, the thermographic measurements based on the measurement of infrared radiation emitted from the surface of the structure, the entire surface was covered with an even layer to elimination of reflections (3D Anti-Glare Spray, Helling company) in order to align the emissivity of the whole surface. In the first step, the temperature was measured for several points on the structure. Moreover, by measuring the temperature for the

whole area of the structure the average, maximum and minimum temperatures were determined. Measurements were also performed for the model with attached heat sink (the aluminum plate with  $100 \times 100 \times 1 \text{ mm}^3$  dimension). During such measurements the structure was placed on four needle probes (Fig. 4) with heat-sink put on this structure (Fig. 5).

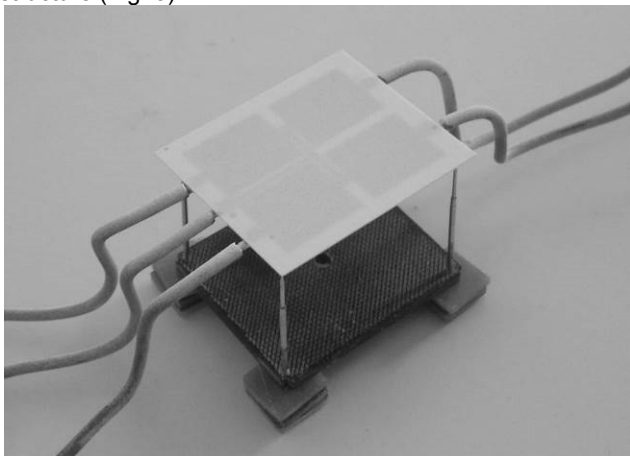


Fig. 4. The measuring set-up

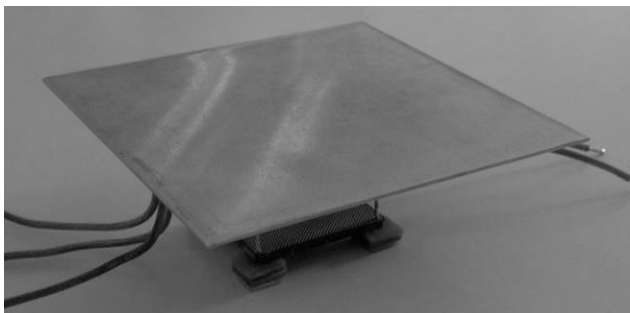


Fig. 5. The aluminum heat-sink

### Results

Measuring points on the structure and on the heat-sink surfaces are presented in Fig. 6, whereas the results are shown in Figs. 7-14.

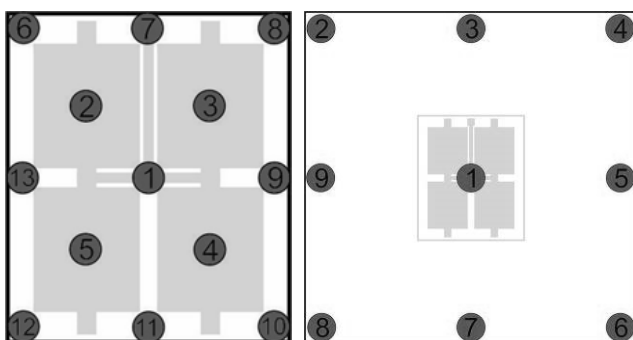


Fig. 6. Measuring points of the structure (left) and heat-sink surface (right)

The markings on the graphs: the digit before the dot is the measuring point shown in Fig. 6, the digit after dot - configuration (Fig. 3). Example of temperature changes on the structure in point 1 for heating and cooling are shown in Fig. 7 (structure no 1) and 8 (structure no 2), while on the heat-sink in point 1 are shown in Fig. 9 (with structure no 1) and 10 (with structure no 2).

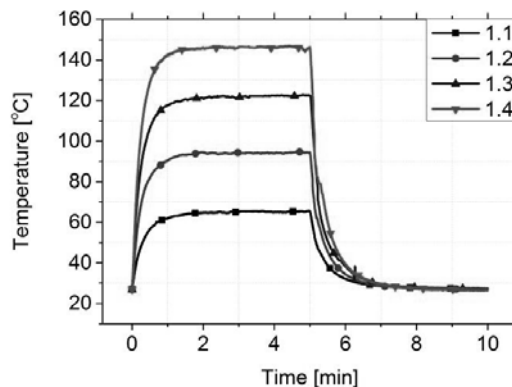


Fig. 7. Temperature changes on the structure no 1 (point 1) during heating and cooling

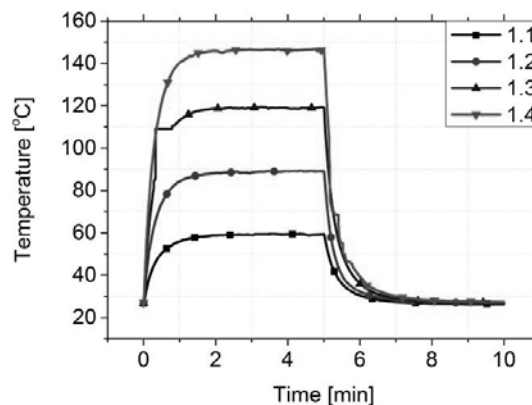


Fig. 8. Temperature changes on the structure no 2 (point 1) during heating and cooling

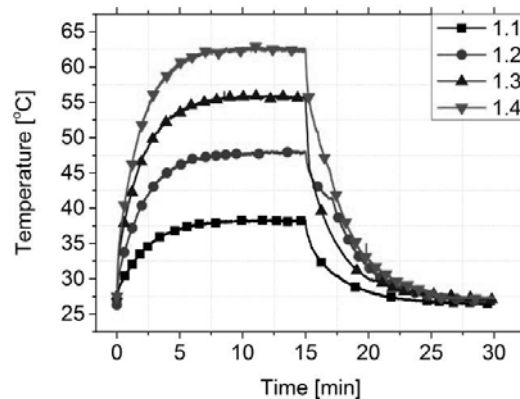


Fig. 9. Temperature changes on the heat-sink with structure no 1 (point 1) during heating and cooling

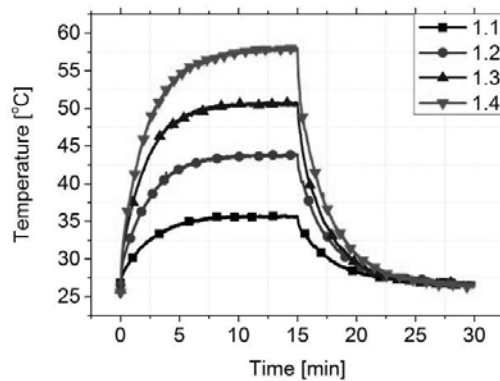


Fig. 10. Temperature changes on the heat-sink with structure no 2 (point 1) during heating and cooling

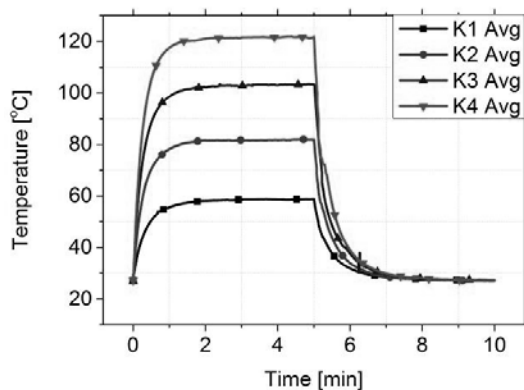


Fig. 11. Temperature changes on the structure no 1 (average value of whole area) during heating and cooling

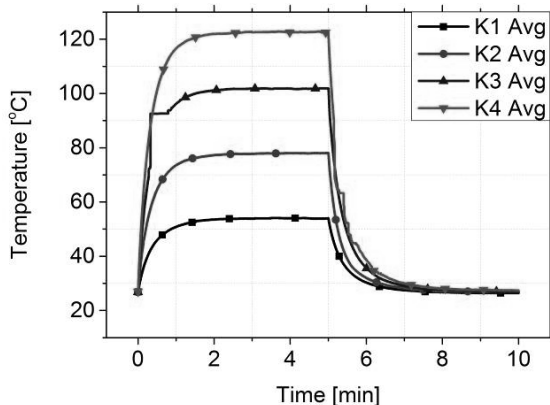


Fig. 12. Temperature changes on the structure no 2 (average value of whole area) during heating and cooling

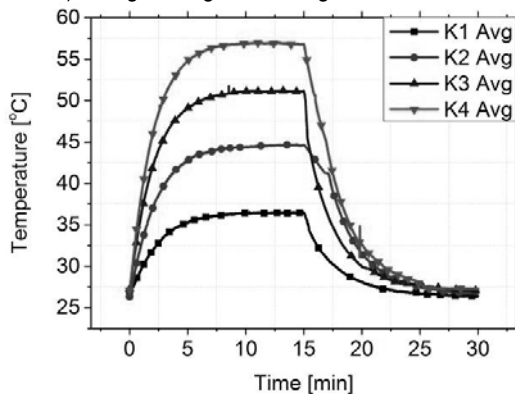


Fig. 13. Temperature changes on the heat-sink with structure no 1 (average value of whole area) during heating and cooling

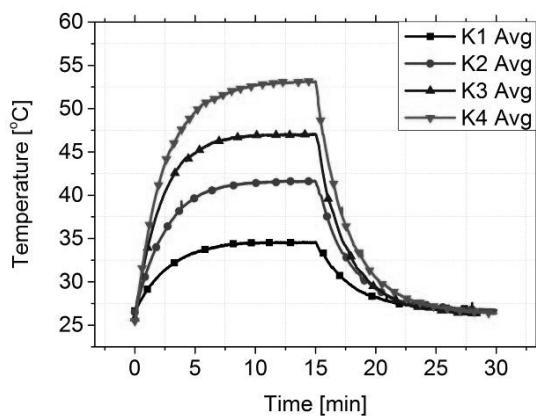


Fig. 14. Temperature changes on the heat-sink with structure no 2 (average value of whole area) during heating and cooling

Thermovision system allowed measurement of the average temperature of the whole areas (both for structure as well as for heat-sink). Average value of temperature on the structure for heating and cooling are shown in Fig. 11 (structure no 1) and 12 (structure no 2), while on the heat-sink are shown in Fig. 13 (with structure no 1) and 14 (with structure no 2).

Pictures from the thermovision camera show the temperature distribution after stabilization for all configurations, heating structure are shown in Figs. 15-18, whereas heating of structure with heat-sink are shown in Figs. 19-22. Pictures of structure without heat-sink perfectly illustrate the place of the heated resistors (cores).



Fig. 15. Thermovision camera views of the structure for "K1" configuration

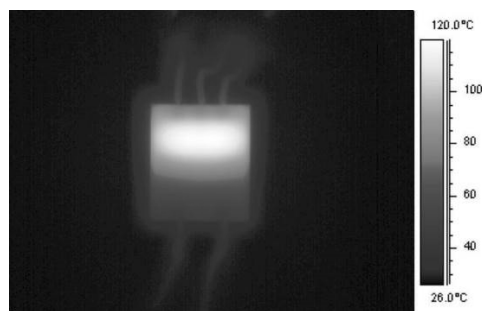


Fig. 16. Thermovision camera views of the structure for "K2" configuration

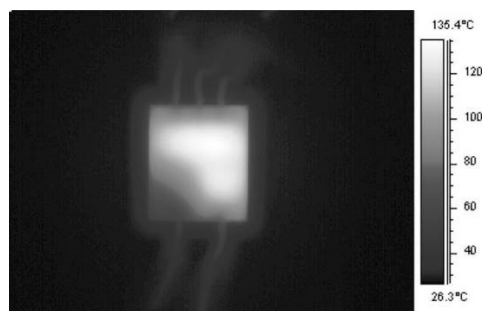


Fig. 17. Thermovision camera views of the structure for "K3" configuration

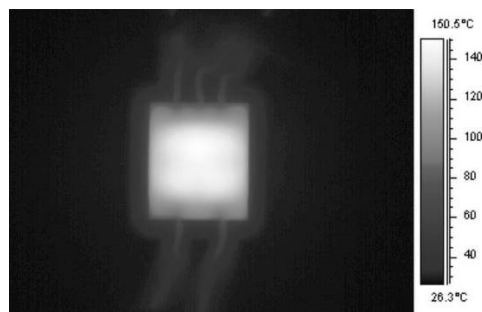


Fig. 18. Thermovision camera views of the structure for "K4" configuration

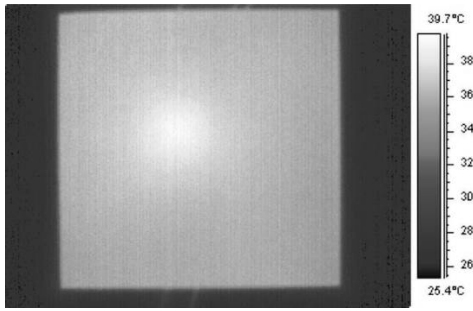


Fig. 19. Thermovision camera views of the heat-sink surfaces for "K1" configuration

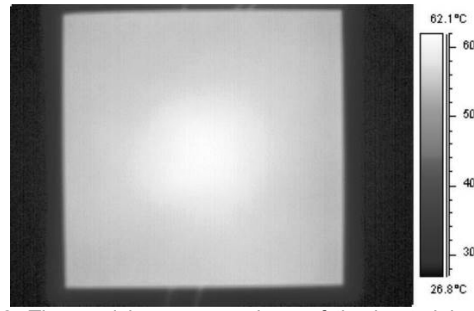


Fig. 22. Thermovision camera views of the heat-sink surfaces for "K4" configuration

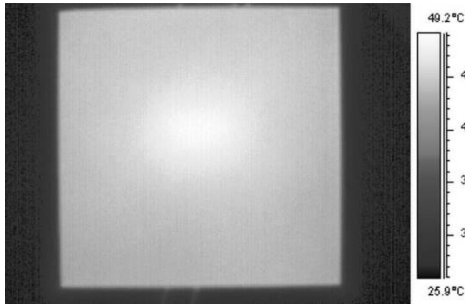


Fig. 20. Thermovision camera views of the heat-sink surfaces for "K2" configuration

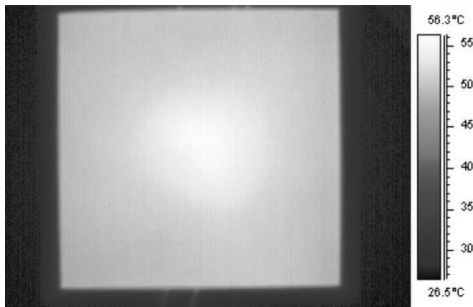


Fig. 21. Thermovision camera views of the heat-sink surfaces for "K3" configuration

### Summary

The temperature rises fairly evenly with the number of heaters (change configuration). Characteristics of heating and cooling of both structures are very similar, also for temperature distribution in a heat-sink surface. ESL 2611-SP and DuPont 2021 pastes are suitable for this type of solutions. The structure with the four resistors allows simulating thermal behavior of quad-processor, and thus continuing the work related to the project.

*Acknowledgment: This work was supported by the National Science Center (Poland), Grant no DEC-2014/13/B/ST7/016.*

**Authors:** mgr inż. Mirosław Gierczak, E-mail: [miroslaw.gierczak@pwr.edu.pl](mailto:miroslaw.gierczak@pwr.edu.pl), mgr inż. Krzysztof Stojek, E-mail: [krzysztof.stojek@pwr.edu.pl](mailto:krzysztof.stojek@pwr.edu.pl), prof. dr hab. inż. Andrzej Dzedzic, E-mail: [andrzej.dzedzic@pwr.edu.pl](mailto:andrzej.dzedzic@pwr.edu.pl), Politechnika Wroclawska, Wydział Elektroniki Mikrosystemów i Fotoniki, Wybrzeże Wyspiańskiego 27, 50-370 Wrocław.

### REFERENCES

- [1] Samake A., Kocanda P., Kos A., Improvement of microsystem throughput using new cooling system, Zeszyty Naukowe Politechniki Rzeszowskiej 294, Elektrotechnika 35 (2016), pp. 5-15
- [2] <http://www.dupont.com/content/dam/dupont/products-and-services/electronic-and-electrical-materials/documents/prodlib/2000.pdf>
- [3] Gierczak M., Markowski P., Dzedzic A., Modeling, Simulation and Analysis of Temperature Distribution in a Heat Sink, IEEE, 2016 39th International Spring Seminar on Electronics Technology (ISSE), pp. 122-127